Supplementary Information

In-situ Recrystallization of Zero-Dimensional Hybrid Metal Halide Glass-Ceramics Toward Improved Scintillation Performance

Bohan Li,[a] Jiance Jin,[b] Meijuan Yin,[a] Kai Han,[b] Yuchi Zhang,[a] Xinlei Zhang,[a] Anran Zhang,[b] Zhiguo Xia*[b] and Yan Xu*[a]

[a]*Department of Chemistry, College of Sciences, Northeastern University, Shenyang, 110819, China. E-mail: xuyan@mail.neu.edu.cn (Y. Xu)*
[b] *State Key Laboratory of Luminescent Materials and Devices, Guangdong Provincial Key Laboratory of Fiber Laser Materials and Applied Techniques, School of Materials Science and Engineering, South China University of Technology, Guangzhou, 510641, China.Email: xiazg@scut.edu.cn*

***Corresponding Authors:**
xuyan@mail.neu.edu.cn (Y. Xu);
xiazg@scut.edu.cn (Z. G. Xia)

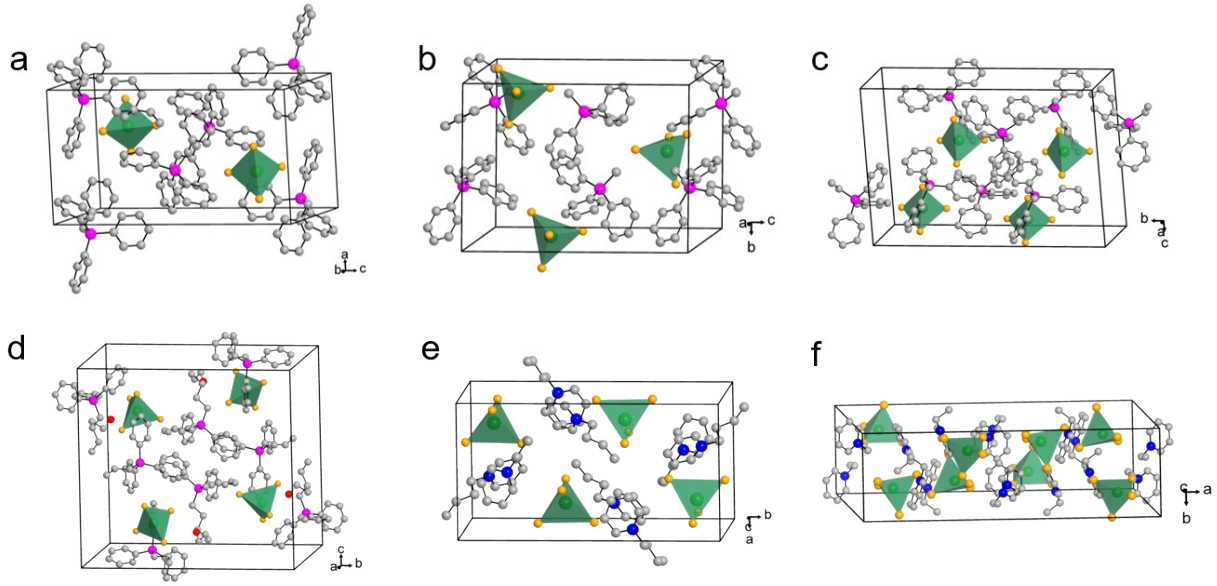

Supplementary Figure 1 Crystal structure of $(BTP)_2MnBr_4$ (a), $(MTP)_2MnBr_4$ (b), $(ETP)_2MnBr_4$ (c), $(BuTP)_2MnBr_4$ (d), $(1\text{-}EP)_2MnBr_4$ (e), and $(1\text{-}BuP)_2MnBr_4$ (f).

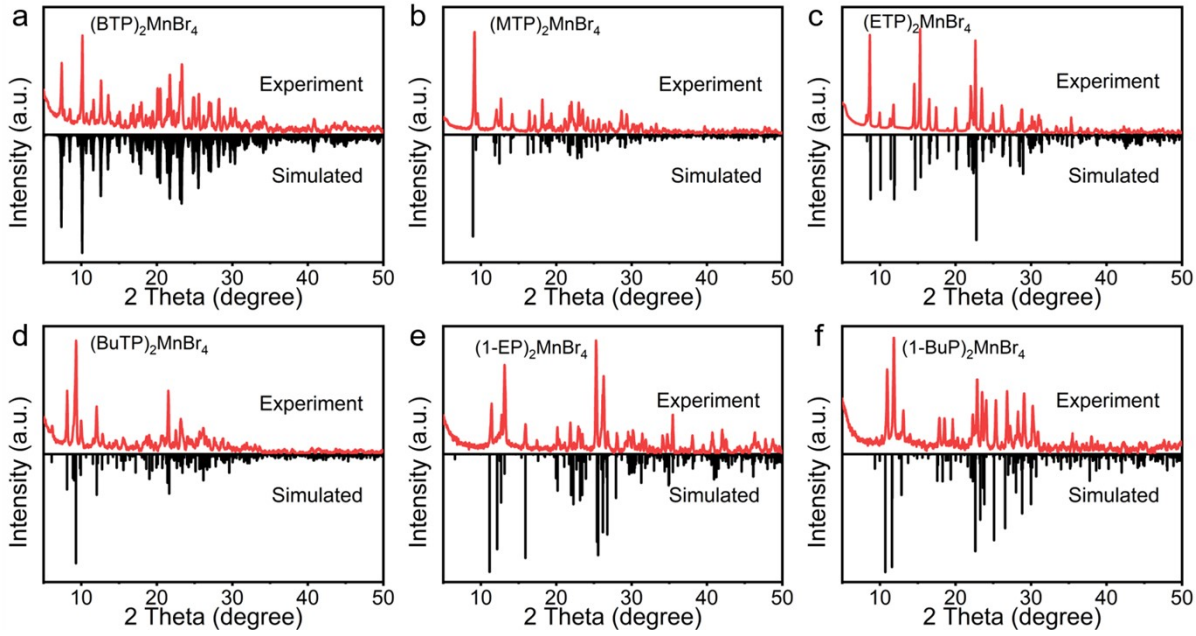

Supplementary Figure 2 Simulated and experimental PXRD patterns for $(BTP)_2MnBr_4$ (a), $(MTP)_2MnBr_4$ (b), $(ETP)_2MnBr_4$ (c) $(BuTP)_2MnBr_4$ (d), $(1\text{-}EP)_2MnBr_4$ (e), and $(1\text{-}BuP)_2MnBr_4$ (f) crystal.

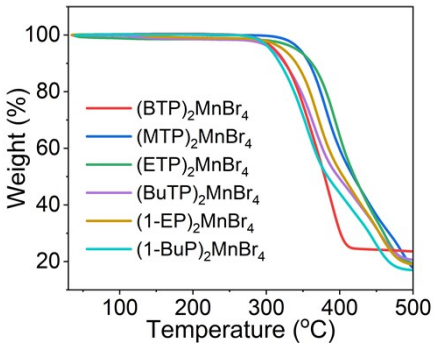

Supplementary Figure 3 TGA curve of $(BTP)_2MnBr_4$, $(MTP)_2MnBr_4$, $(ETP)_2MnBr_4$, $(BuTP)_2MnBr_4$, $(1\text{-}EP)_2MnBr_4$, $(1\text{-}BuP)_2MnBr_4$ crystal.

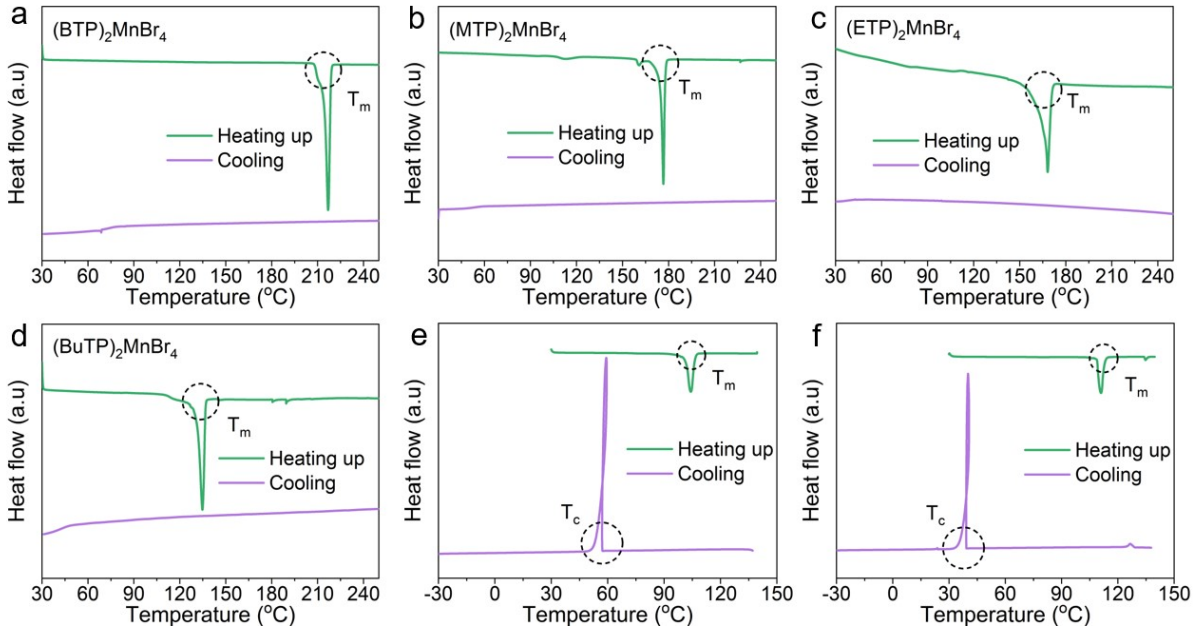

Supplementary Figure 4 Heating up and cooling scans for $(BTP)_2MnBr_4$ (a), $(MTP)_2MnBr_4$ (b), $(ETP)_2MnBr_4$ (c), $(BuTP)_2MnBr_4$ (d), $(1\text{-}EP)_2MnBr_4$ (e), $(1\text{-}BuP)_2MnBr_4$ (f) crystals.

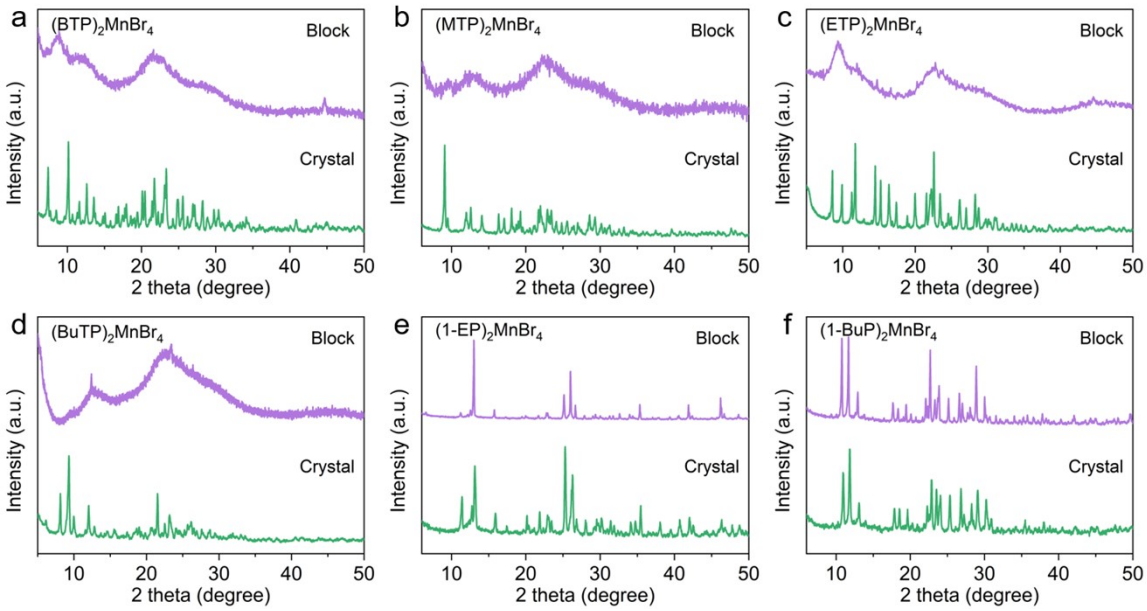

Supplementary Figure 5. PXRD patterns for $(BTP)_2MnBr_4$ (a), $(MTP)_2MnBr_4$ (b), $(ETP)_2MnBr_4$ (c), $(BuTP)_2MnBr_4$ (d), $(1\text{-}EP)_2MnBr_4$ (e), $(1\text{-}BuP)_2MnBr_4$ (f) crystal and block.

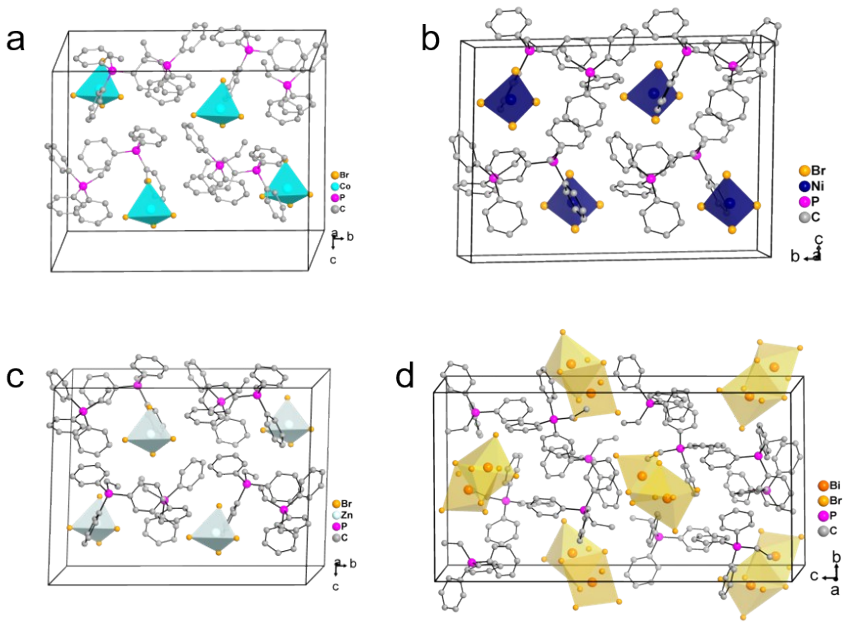

Supplementary Figure 6 Crystal structure of $(ETP)_2CoBr_4$ (a), $(ETP)_2NiBr_4$ (b), $(ETP)_2ZnBr_4$ (c) and $(ETP)_3Bi_2Br_9$ (d).

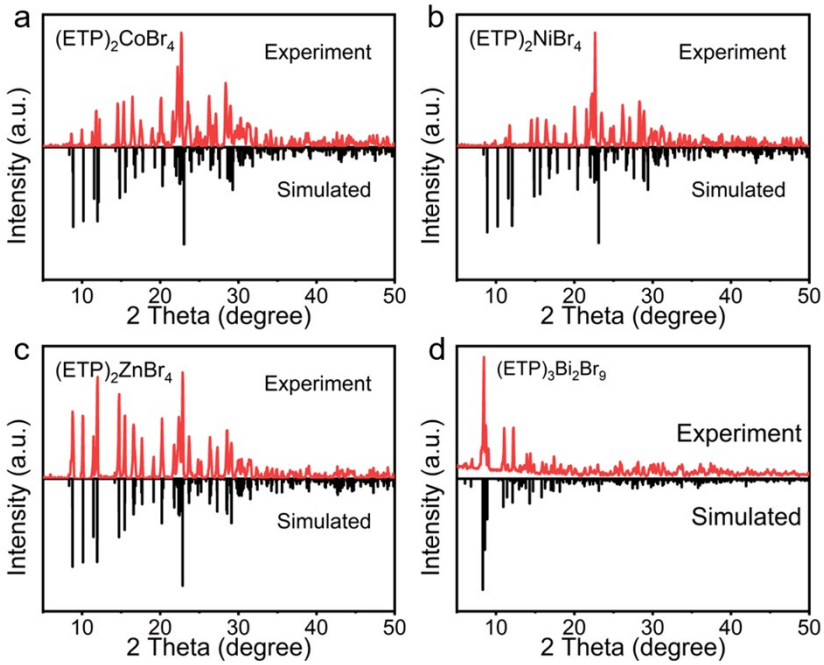

Supplementary Figure 7 Simulated and experimental PXRD patterns for $(ETP)_2CoBr_4$ (a), $(ETP)_2NiBr_4$ (b), $(ETP)_2ZnBr_4$ (c) and $(ETP)_3Bi_2Br_9$ (d) crystal.

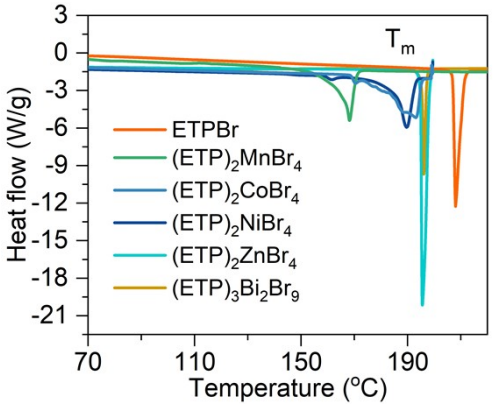

Supplementary Figure 8 DSC up-scans for ETPBr, $(ETP)_2MnBr_4$, $(ETP)_2CoBr_4$, $(ETP)_2NiBr_4$, $(ETP)_2ZnBr_4$, $(ETP)_3Bi_2Br_9$ crystals.

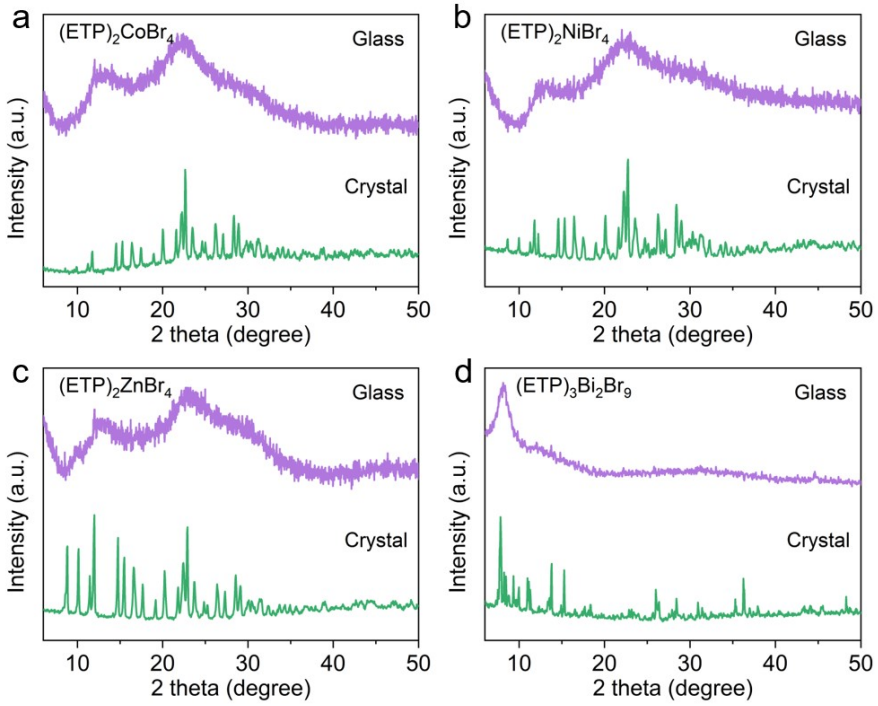

Supplementary Figure 9 PXRD patterns for $(ETP)_2CoBr_4$ (a), $(ETP)_2NiBr_4$ (b), $(ETP)_2ZnBr_4$ (c), $(ETP)_3Bi_2Br_9$ (d) crystal and glass.

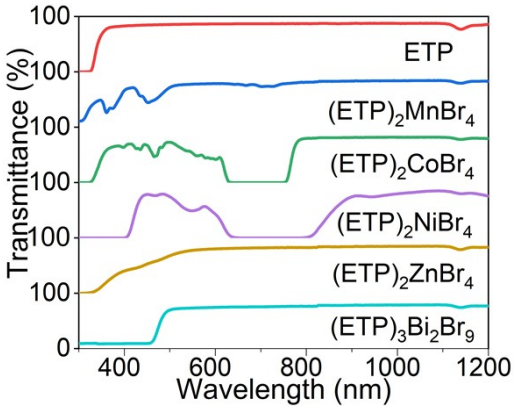

Supplementary Figure 10 Light transmittance of ETP, $(ETP)_2MnBr_4$, $(ETP)_2CoBr_4$, $(ETP)_2NiBr_4$, $(ETP)_2ZnBr_4$, $(ETP)_3Bi_2Br_9$ glass.

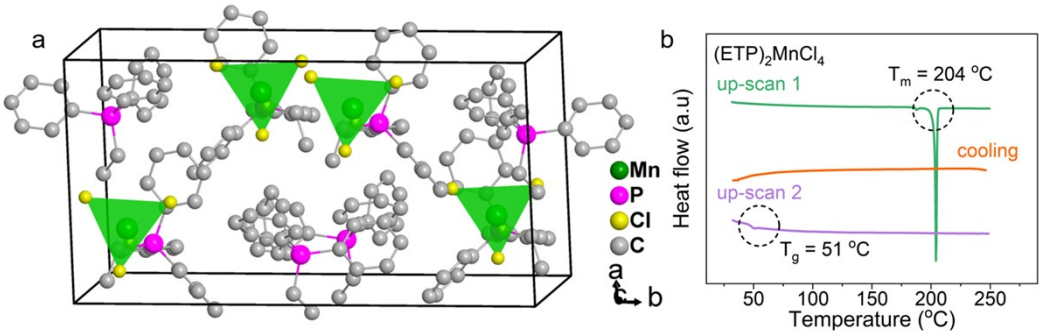

Supplementary Figure 11 Crystal structure (a) and DSC curve (b) for $(ETP)_2MnCl_4$.

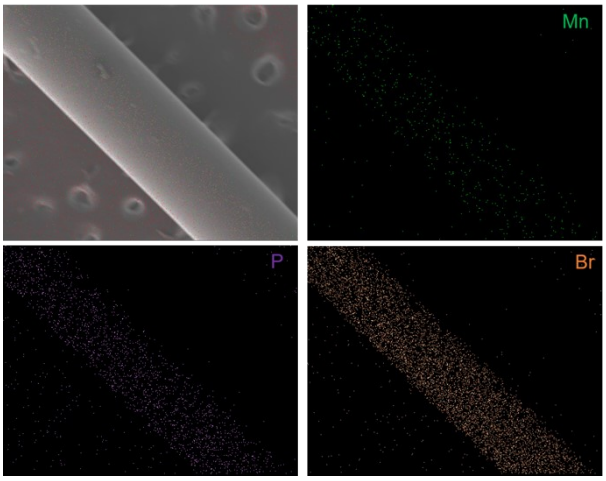

Supplementary Figure 12 SEM image of $(BTP)_2MnBr_4$ optical fiber and elemental mapping of P, Mn and Br.

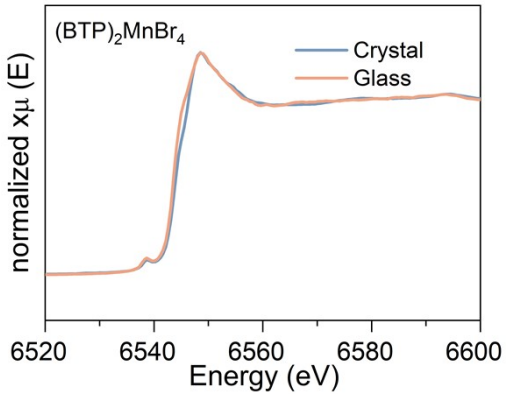

Supplementary Figure 13 Normalized XANES profiles recorded at the Mn K-edges of the $(BTP)_2MnBr_4$ crystal and glass.

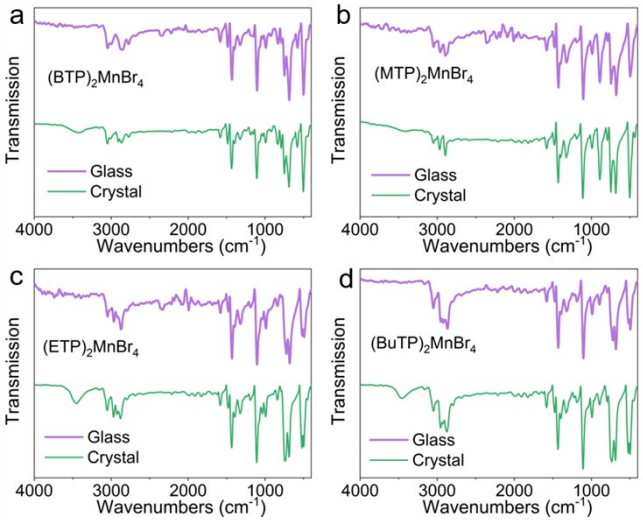

Supplementary Figure 14 FTIR spectra of $(BTP)_2MnBr_4$ (a), $(MTP)_2MnBr_4$ (b), $(ETP)_2MnBr_4$ (c), $(BuTP)_2MnBr_4$ (d) crystal and glass.

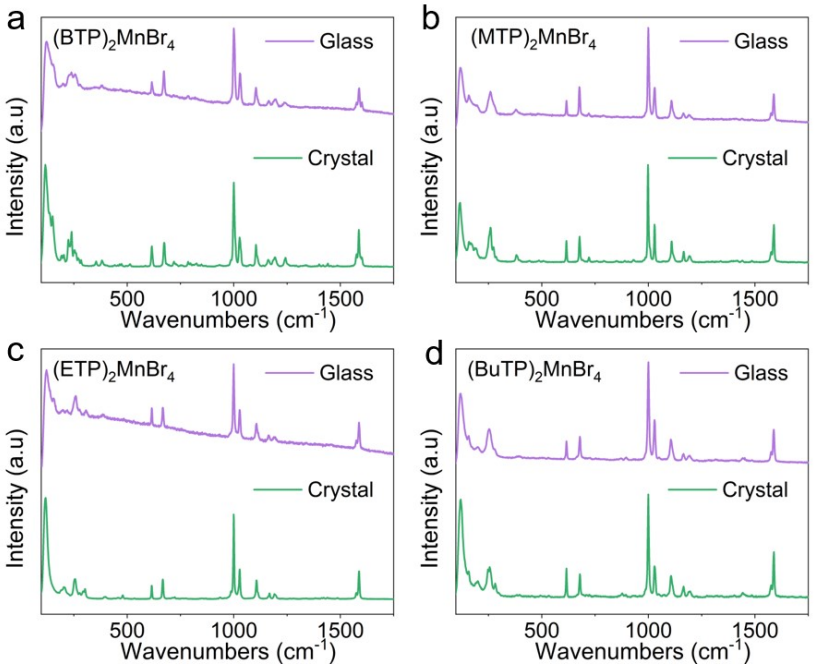

Supplementary Figure 15 Raman spectra of $(BTP)_2MnBr_4$ (a), $(MTP)_2MnBr_4$ (b), $(ETP)_2MnBr_4$ (c), $(BuTP)_2MnBr_4$ (d) crystal and glass.

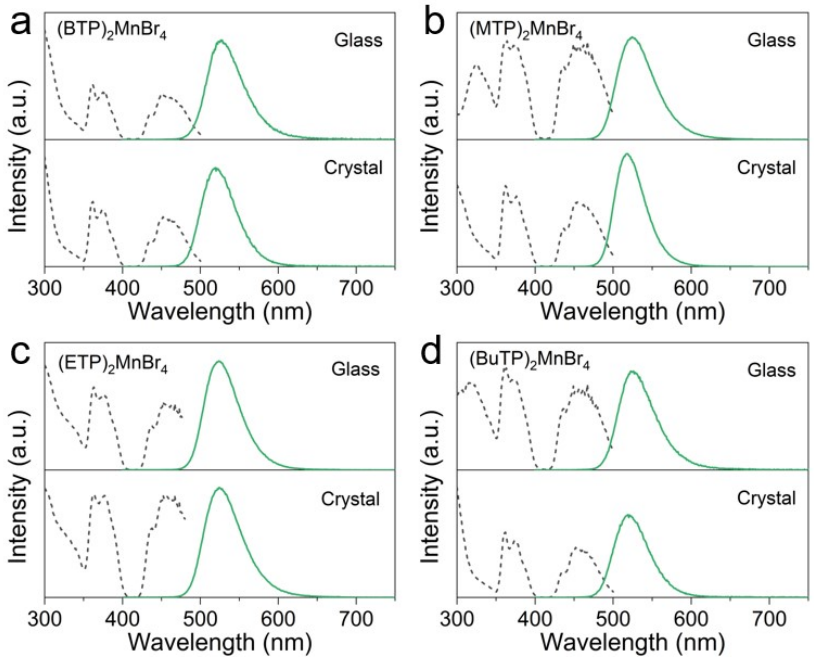

Supplementary Figure 16 PLE and PL spectra of $(BTP)_2MnBr_4$ (a), $(MTP)_2MnBr_4$ (b), $(ETP)_2MnBr_4$ (c), $(BuTP)_2MnBr_4$ (d) crystal and glass.

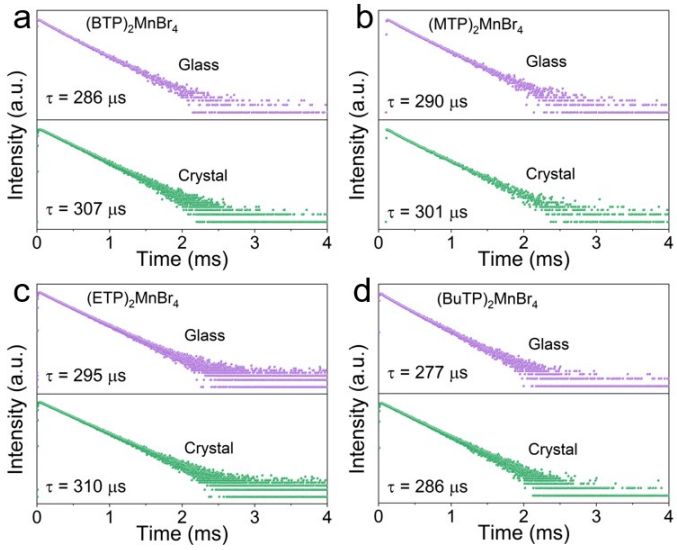

Supplementary Figure 17 Luminescence decay curve of $(BTP)_2MnBr_4$ (a), $(MTP)_2MnBr_4$ (b), $(ETP)_2MnBr_4$ (c), $(BuTP)_2MnBr_4$ (d) crystal and glass.

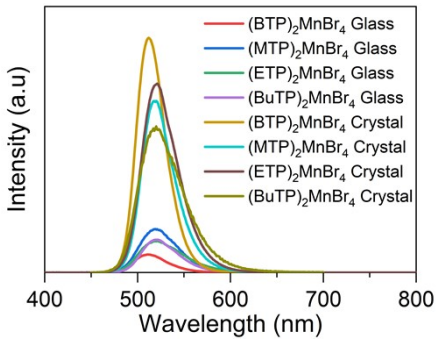

Supplementary Figure 18 Radioluminescence spectra of $(BTP)_2MnBr_4$, $(MTP)_2MnBr_4$, $(ETP)_2MnBr_4$, $(BuTP)_2MnBr_4$ crystal and glass.

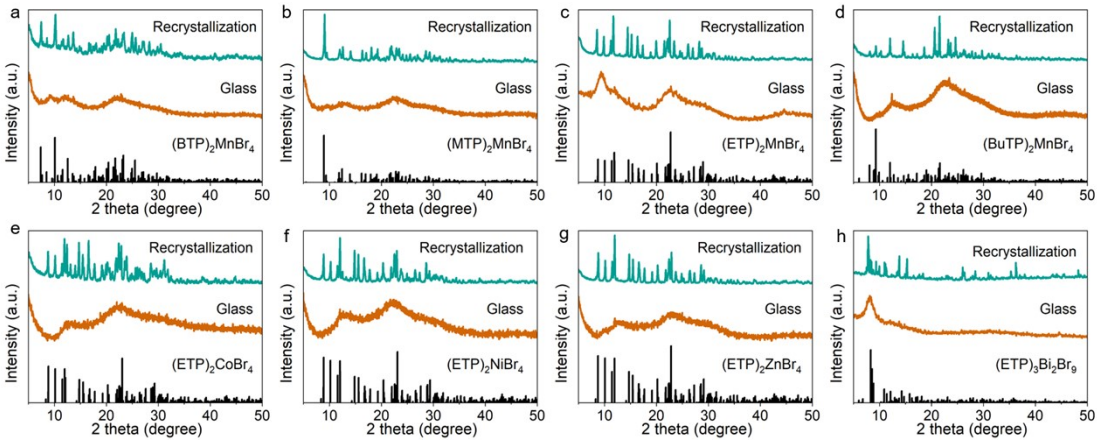

Supplementary Figure 19 XRD pattern of $(BTP)_2MnBr_4$ (a), $(MTP)_2MnBr_4$ (b), $(ETP)_2MnBr_4$ (c), $(BuTP)_2MnBr_4$ (d), $(ETP)_2CoBr_4$ (e), $(ETP)_2NiBr_4$ (f), $(ETP)_2ZnBr_4$ (g) and $(ETP)_3Bi_2Br_9$ (h)comparison of glass recrystallized with glass.

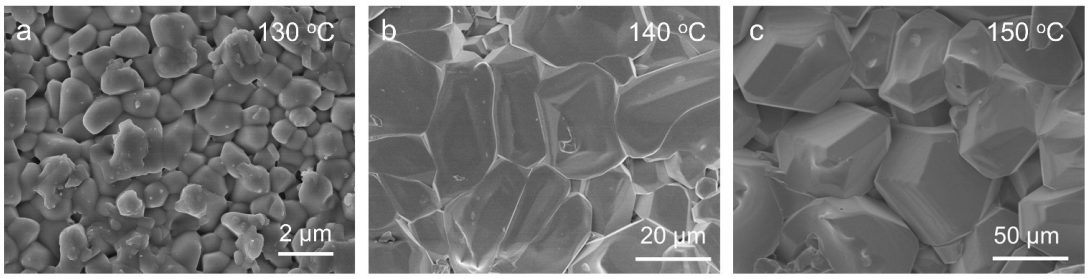

Supplementary Figure 20 SEM images of $(BTP)_2MnBr_4$ G-Cs crystallized at 130 °C (a), 140 °C (b), 150 °C (c).

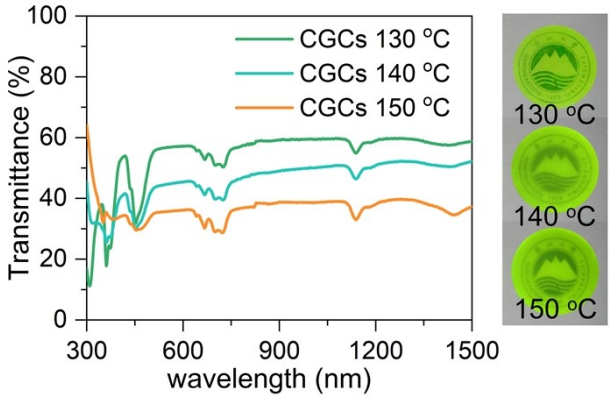

Supplementary Figure 21 Light transmittance of $(BTP)_2MnBr_4$ G-Cs crystallized at 130 °C, 140 °C, 150 °C.

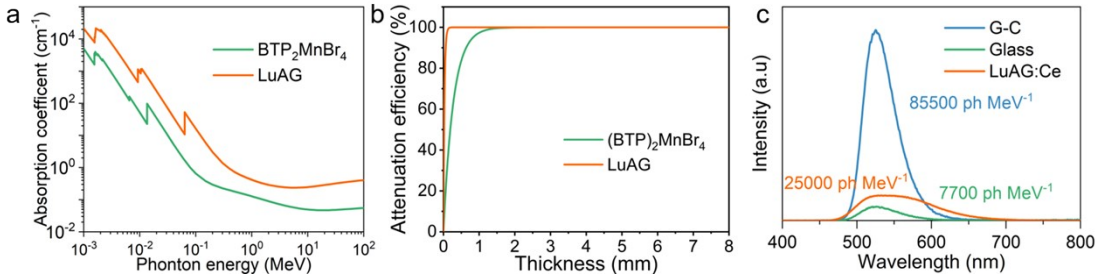

Supplementary Figure 22 (a) Absorption coefficients of LuAG:Ce and $(BTP)_2MnBr_4$ as a function of photon energy from 1 keV to 100 MeV. (b) Attenuation efficiency of LuAG:Ce and $(BTP)_2MnBr_4$ as a function of photon energy 17.5 KeV. (c) X-ray radio luminescence (RL) spectra of $(BTP)_2MnBr_4$ glass, $(BTP)_2MnBr_4$ G-C and LAG:Ce under X-ray irradiation.

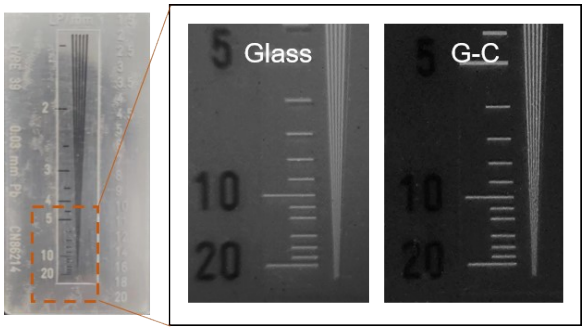

Supplementary Figure 23 X-ray image of the standard X-ray resolution pattern plate.

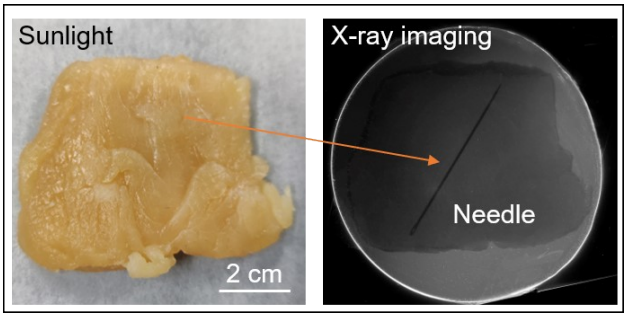

Supplementary Figure 24 Daylight photograph and X-ray image of chicken with needle inserted.

Supplementary Table 1. The crystal structure parameters of $(C_{25}H_{22}P)_2MnBr_4$, $(C_{19}H_{18}P)_2MnBr_4$, $(C_{20}H_{20}P)_2MnBr_4$ and $(C_{22}H_{24}P)_2MnBr_4{\cdot}C_2H_5OH$.

Formula	$C_{50}H_{44}Br_4MnP_2$ (CCDC 2285876)	$C_{38}H_{36}Br_4MnP_2$ (CCDC 2285882)	$C_{40}H_{40}Br_4MnP_2$ (CCDC 2169124)	$C_{46}H_{54}Br_4MnOP_2$ (CCDC 2285877)
Dimension (mm)	0.2 × 0.18 × 0.16	0.2 × 0.18 × 0.16	0.2 × 0.18 × 0.16	0.2 × 0.18 × 0.16
Molecular weight	1081.37	929.19	957.24	1059.41
Temperature (K)	301	273	150	293
Crystal system	Triclinic	monoclinic	monoclinic	monoclinic
Space group	*P-1*	$P2_1$	*C*1*c*1	$P2_1$
Z	2	2	4	4
a (Å)	10.4567 (3)	9.7924 (2)	12.2698 (7)	10.8592 (2)
b (Å)	12.5204 (3)	12.5306 (2)	21.2817 (11)	21.7967 (5)
c (Å)	18.4226 (5)	16.6305 (3)	16.3853 (11)	19.6633 (5)
α (°)	105.994 (2)	90	90	90
β (°)	92.776 (2)	105.085 (2)	110.717 (2)	96.743 (1)
γ (°)	92.767 (2)	90	90	90
V (Å^3)	2311.07 (11)	1970.32 (6)	4001.9 (4)	4622.01 (18)
ρ_{calc} (g/cm^3)	1.554	1.566	1.589	1.522
μ (mm^{-1})	7.277	8.425	4.430	3.846
Reflections measured	23657	12550	34259	44228
Reflections independent	8929	5843	8146	10611
R_{int}	0.0219	0.0198	0.0624	0.0483
R_1 [I > 2sigma(I)][a]	0.0300	0.0249	0.0485	0.0366
$wR(F^2)$·[I > 2sigma(I)][b]	0.0746	0.0655	0.1151	0.0727
Goof	1.051	1.058	1.071	1.017

[a] $R_1 = \sum \| F_o| - |F_c \| / \sum |F_o|$, [b] $wR_2 = [\sum w(F_o^2 - F_c^2)^2 / \sum w(F_o^2)^2]^{1/2}$

Supplementary Table 2. The crystal structure parameters of $(C_{20}H_{20}P)_2CoBr_4$, $(C_{20}H_{20}P)_2NiBr_4$, $(C_{20}H_{20}P)_2ZnBr_4$ and $(C_{20}H_{20}P)_3Bi_2Br_9$.

Formula moiety	$C_{40}H_{40}Br_4CoP_2$ (CCDC-2285878)	$C_{40}H_{40}Br_4NiP_2$ (CCDC 2285879)	$C_{40}H_{40}Br_4ZnP_2$ (CCDC 2285880)	$C_{60}H_{60}Bi_2Br_9P_3$ (CCDC 2285881)
Dimension (mm)	0.2 × 0.18 × 0.16	0.2 × 0.18 × 0.16	0.2 × 0.18 × 0.16	0.2 × 0.18 × 0.16
Molecular weight	961.23	961.01	967.67	2011.14
Temperature (K)	293	293	300	300
Crystal system	Monoclinic	Monoclinic	Monoclinic	Orthorhombic
Space group	*C*1*c*1	*C*1*c*1	*Cc*	$P2_12_12_1$
Z	4	4	4	4
a (Å)	12.2214 (5)	12.1800 (5)	12.3305 (2)	14.5071 (10)
b (Å)	21.1041 (5)	21.0104 (5)	21.1916 (3)	15.5088 (10)
c (Å)	16.4141 (7)	16.4238 (7)	16.6153 (3)	29.2071 (3)
α (°)	90	90	90	90
β (°)	111.1290 (10)	111.4920 (10)	111.612 (2)	90
γ (°)	90	90	90	90
V (Å^3)	3948.9 (3)	3910.7 (3)	4036.41 (12)	6571.24 (9)
ρ_{calc} (g/cm^3)	1.617	1.632	1.592	2.033
μ (mm^{-1})	4.590	4.692	6.429	17.767
Reflections measured	19693	18331	18709	30168
Reflections independent	7800	7454	5958	12478
R_{int}	0.0384	0.0337	0.0177	0.0247
R_1 [I > 2sigma(I)][a]	0.0573	0.0421	0.0375	0.0337
$wR(F^2)$·[I > 2sigma(I)][b]	0.1521	0.0968	0.0982	0.0885
Goof	1.030	1.027	1.094	1.069

[a] $R_1 = \sum \| F_o| - |F_c \| / \sum |F_o|$, [b] $wR_2 = [\sum w(F_o^2 - F_c^2)^2 / \sum w(F_o^2)^2]^{1/2}$

Supplementary Table 3. The crystal structure parameters of $(ETP)_2MnCl_4$.

Formula	$C_{40}H_{40}Cl_4MnP_2$ (CCDC 2285898)
Dimension (mm)	0.2 × 0.2 × 0.2
Molecular weight	779.40
Temperature (K)	293
Crystal system	Monoclinic
Space group	*C*1*c*1
Z	4
a (Å)	12.1993 (2)
b (Å)	20.8825 (3)
c (Å)	16.3635 (3)
α (°)	90
β (°)	110.775 (2)
γ (°)	90
V (Å^3)	3897.59 (12)
ρ_{calc} (g/cm^3)	1.328
μ (mm^{-1})	6.254
Reflections measured	11188
Reflections independent	4819
R_{int}	0.0219
R_1 [I > 2sigma(I)][a]	0.0303
$wR(F^2)\cdot$[I > 2sigma(I)][b]	0.0833
Goof	1.082

[a] $R_1 = \sum \| F_o| - |F_c \| / \sum |F_o|$, [b] $wR_2 = [\sum w(F_o^2 - F_c^2)^2 / \sum w(F_o^2)^2]^{1/2}$

Supplementary Table 4. Summary of EXAFS fitting parameters for $(BTP)_2MnBr_4$ crystal and glass.

Sample	Bond	Coordination No.	R
Crystal	Mn-Br	3	2.63 Å
	Mn-Br	1	2.56 Å
Glass	Mn-Br	3	2.53 Å
	Mn-Br	1	2.63 Å

Supplementary Table 5. PLQY of $(BTP)_2MnBr_4$, $(MTP)_2MnBr_4$, $(ETP)_2MnBr_4$, $(BuTP)_2MnBr_4$ crystal and glass.

Sample	$(BTP)_2MnBr_4$	$(MTP)_2MnBr_4$	$(ETP)_2MnBr_4$	$(BuTP)_2MnBr_4$
Crystal	98%	97%	96%	92%
Glass	48%	57%	57%	50%